analytical chemistry

Article

pubs.acs.org/ac

# Reversible Photoswitching of Spiropyran-Conjugated Semiconducting Polymer Dots

Yang-Hsiang Chan,[†] Maria Elena Gallina,[†] Xuanjun Zhang, I-Che Wu, Yuhui Jin, Wei Sun, and Daniel T. Chiu*

Department of Chemistry, University of Washington, Seattle, Washington 98195, United States

Supporting Information

**ABSTRACT:** Semiconducting polymer dots (Pdots) recently have emerged as a new class of ultrabright fluorescent probes with promising applications in biological detection and imaging. We developed photoswitchable Pdots by conjugating photochromic spiropyran molecules onto poly[9,9-dioctylfluorenyl-2,7-diyl)-*co*-1,4-benzo-{2,1′-3}-thiadiazole)] (PFBT). The modulation of fluorescence was achieved by ultraviolet irradiation, which converted spiropyran into its visible-absorbing merocyanine form. The merocyanine efficiently quenched the fluorescence of PFBT via Förster resonance energy transfer (FRET). We then reversed the quenching by subsequent irradiation with visible light to get back the fluorescence of PFBT. This FRET-based photomodulation of Pdot fluorescence could be repeated multiple times. We next conjugated biomolecules onto the surface of these photoswitchable Pdots and demonstrated their specific cellular and subcellular labeling to different types of cells without any noticeable nonspecific binding. We anticipate these photoswitchable and biocompatible Pdots will be useful in developing bioimaging techniques in the future.

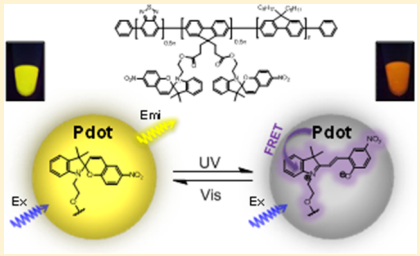


The investigation of biological processes at the single-cell level has attracted much attention in various applications, such as measuring single-cell activity, DNA repair mechanisms, gene regulation, and diagnosis of disease.[1,2] For this reason, the exploration of optical monitoring at molecular scales and the design of sensing devices in complex microenvironments has become a pressing issue. Among the various imaging techniques of biological systems, fluorescence microscopy is, by far, one of the most powerful cellular analysis tools because of its high signal-to-noise ratio, excellent spatial and temporal resolution, and noninvasive nature. Fluorescence microscopy relies on the use of specific labeling at the molecular level, where the fluorophores with desired emission wavelengths are bound to the biological components of interest prior to fluorescence imaging. To obtain sufficient signals from molecules to study biological systems or to improve the spatial resolution of conventional microscopy, there have been great efforts to exploit fluorescence-based probes in recent years.[3−5]

Several super-resolution fluorescence microscopy techniques, including stimulated emission depletion (STED) microscopy,[6,7] saturated structured-illumination microscopy (SSIM),[8] stochastic optical reconstruction microscopy (STORM),[9] and photoactivated localization microscopy (PALM) have been developed and all these methods rely on the use of suitable fluorescent probes.[10] For example, in super-resolution techniques based on the localization of individual fluorophores, such as STORM and PALM, photoswitchable molecules or proteins are used; different subsets of fluorophores are selectively activated or reversibly switched between the on and off states by light at different time points. The accurate positions of numerous fluorophores are determined by iterating the activation/switching process so that a super-resolution image can be constructed. Nowadays the development of photoswitchable systems is of crucial importance for providing the assortment of tools required by the growing number of applications. In biology, beyond their importance in super-resolution imaging, photoswitchable probes are used to determine protein concentration in vivo and for studying protein trafficking in live cells.[11] Photoswitchable fluorophores also act as molecular switches,[12] which can be used either for signal processing or for optical data storage.[13,14]

Several groups recently have developed nanoparticle-based fluorescence photomodulation that utilizes Förster resonance energy transfer (FRET), where the selected pairs of donor and acceptor molecules are incorporated, either covalently or noncovalently, into a polymeric matrix.[15−21] Various strategies, including emulsion polymerization, copolymerization, and core−shell embedding, have been used to build a hydrophobic core with a hydrophilic surface.[16,22,23] In those studies, the photochrome, for example, spiropyran (SP) or diarylethene molecules, served as photoswitchable quencher: Once it was converted to its colored form by the absorption of ultraviolet (UV) light, it efficiently quenched the emission of its partnering fluorophore. The quenching mechanism was generally due to the electron or energy transfer from the fluorophore to the photochrome. The following irradiation with visible light reverted the photochrome to the original colorless form and restored the fluorophore emission to the original intensity.

**Received:** August 5, 2012
**Accepted:** October 4, 2012
**Published:** October 4, 2012

   dx.doi.org/10.1021/ac302245t | *Anal. Chem.* 2012, 84, 9431−9438

**Scheme 1. (A) Preparation of Photoswitchable Pdots;[a] (B) UV-Visible Spectra of SP Form (Solid Black Line) and MC Form (Solid Pink Line) in Methanol Solution and Fluorescence Spectrum (Dash Black Line) of PFBT Pdots in Water; (C) Schematic Representation of Pdot Emission Modulation by SP upon Irradiation of UV-Visible Light**

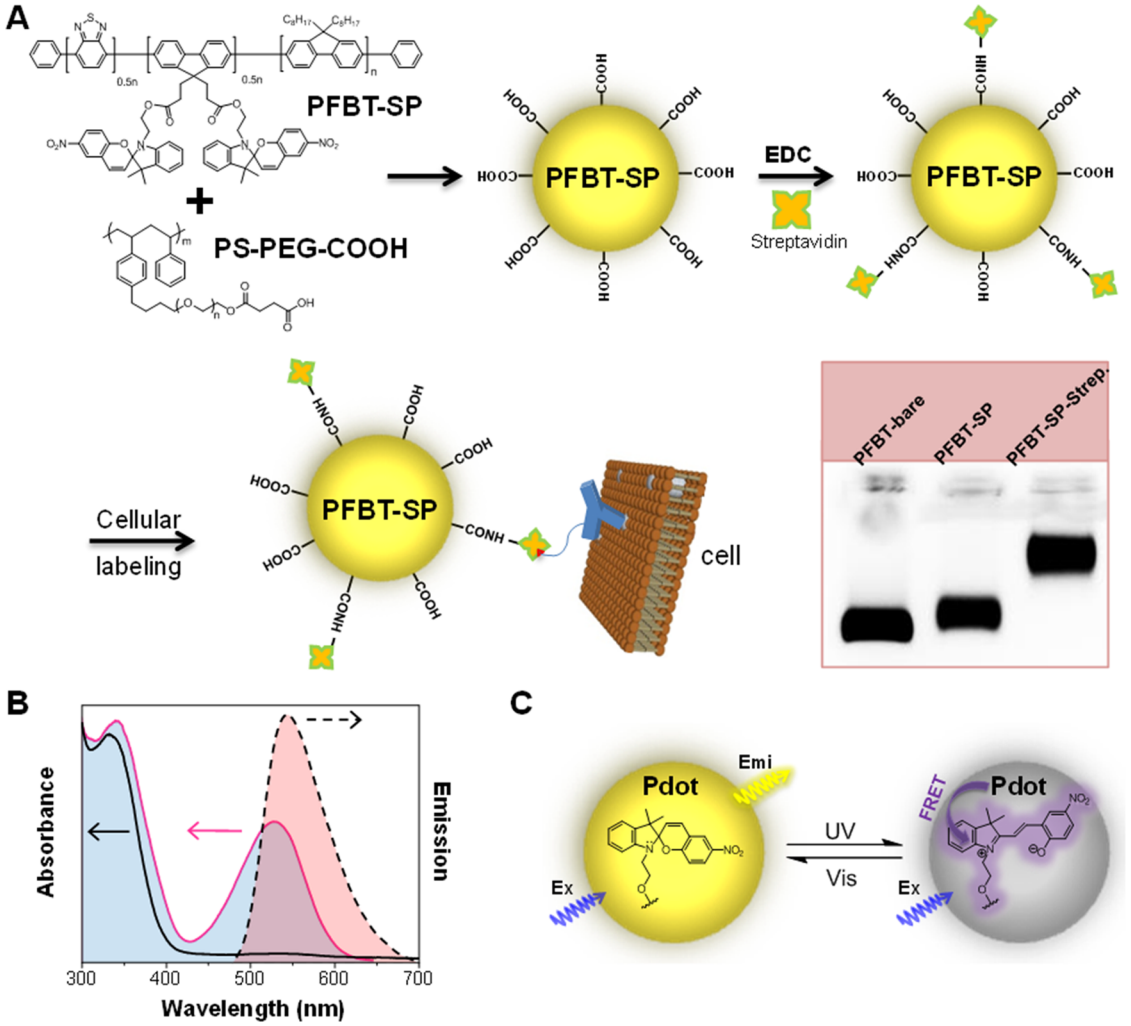


[a]PFBT functionalized with carboxyl groups was first covalently bound by photoswitchable spiropyran (SP) molecules. After the conjugation, the spiropyran-bound PFBT (PFBT-SP) was mixed with PS-PEG-COOH in THF and then co-precipitated in water under vigorous sonication to form photoswitchable Pdots. The photoswitchable Pdots were subsequently conjugated to streptavidin for specific cellular targeting studies. The bottom-right corner shows the electrophoresis of (left to right) bare PFBT dots, PFBT-SP Pdots, and PFBT-SP Pdots after streptavidin conjugation.

Thus, the fluorescence of this fluorophore-photochrome nanoparticle could be switched off and on for multiple cycles by UV and visible light irradiation. For example, Callan and co-workers reported the use of an amphiphilic copolymer that captured a mixture of boron dipyrromethene fluorophores (energy donor) and SP photochromes (energy acceptor) as photoswitchable assemblies.[23] Similarly, Chen et al. used one-step miniemulsion polymerization to attach fluorescent dyes (4-methamino-9-ally-1,8-naphthalimide) and photochromic SP derivatives into individual nanoparticles.[22] In comparison to fluorescent dyes, these nanoparticle-based assemblies were much brighter because many dye molecules were embedded inside a single nanoparticle. All of the studies mentioned above were based on using a central, nonfluorescent matrix, such as latex, polymer, or silica. These optically inert matrices can limit the potential brightness and optical functionality of the final nanoparticle assemblies. To date, there has been a paucity of studies that explore the use of fluorescent nanoparticles (e.g., semiconducting quantum dots) as matrices for fluorescence photomodulation.[24,25] Medintz et al. attached a photochromic dye onto a quantum-dot-coordinated protein to achieve reversible fluorescence photomodulation,[25] but sometimes the potential leakage of the inorganic component and the difficulties in modifying the surfaces of quantum dots[26−29] are issues that have limited their biological applications. Li and co-workers have developed a series of SP-based photoswitchable nanoparticles by taking advantage of the strong fluorescence of the light-induced merocyanine (MC) form when it resides in the hydrophobic environment.[30−34] These nanoparticles have shown promising applications in nanoscopic imaging,[32,34] but their relatively large size (>50 nm) might limit the spatial resolution normally achieved by super-resolution imaging techniques.

Semiconducting polymer dots exhibit exceptional fluorescence brightness, good photostability, fast radiative rate, facile surface functionalization, and low cytotoxicity.[35−41] We have shown that Pdots are biocompatible and can be used for a number of applications both in vitro or in vivo.[42−47] Moreover,


dx.doi.org/10.1021/ac302245t | Anal. Chem. 2012, 84, 9431−9438

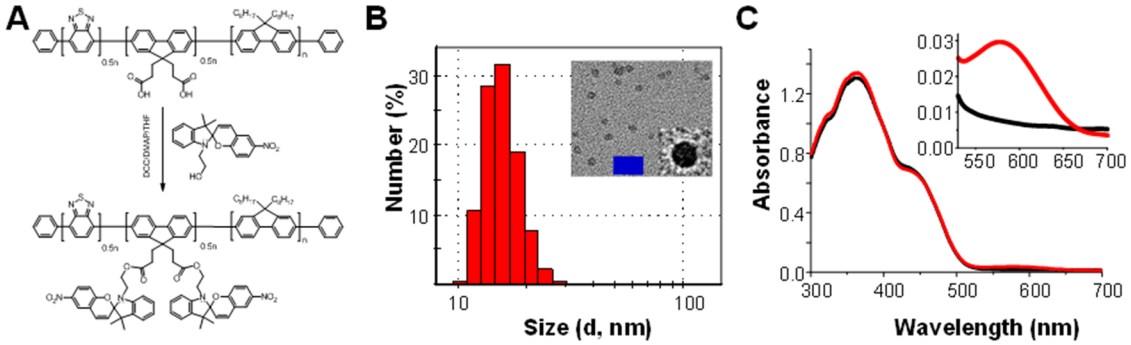


**Figure 1.** (A) Conjugation of hydroxyl-functionalized SP to carboxyl-functionalized PFBT. (B) Hydrodynamic diameters of PFBT-SP Pdots (average diameter was ~16 nm) measured by dynamic light scattering. The inset shows the transmission electron microscopy images, while the upper-right corner inside the inset shows the enlarged view of a single Pdot. Scale bar represents 100 nm. (C) Absorption spectra of PFBT-SP Pdots before (black line) and after (red line) UV light irradiation. The inset magnifies the regions of wavelength from 500 to 700 nm.

the amplified energy transfer from the excited Pdot matrix to the acceptor dyes (e.g., photochromic dyes) located in close proximity to the semiconducting polymer can facilitate the design of photoswitchable probes.[36,48] Recently, Harbron et al. physically doped photochromic dyes into two types of semiconductor polymers, poly[2-methoxy-5-(2-ethylhexyloxy)-1,4-phenylenevinylene] (MEH-PPV) and poly[{9,9-dioctyl-2,7-divinylene-fluorenylene}-alt-*co*-{2-methoxy-5-(2-ethylhexyloxy)-1,4-phenylene}] (PFPV).[49,50] They showed that photochromic dye-doped MEH-PPV Pdots exhibited reversible quenching and recovery but the PFPV counterparts suffered from irreversible photobleaching.[50] However, the very low quantum yield of MEH-PPV Pdots (~0.01) makes further applications less feasible. Moreover, for many of these physical doping strategies, the leaching of the embedded dyes from the polymeric assemblies has been a concern.[51,52] Similarly, Osakada and co-workers doped diarylethene into poly[9,9-dioctylfluorenyl-2,7-diyl)-*co*-1,4-benzo-{2,1′-3}-thiadiazole)] (PFBT) nanoparticles with an average particle diameter of 54 nm, and photoswitching was observed in fixed cells labeled by these nanoparticles.[53] But in the strategy of Osakada and co-workers it should be noted that the mass ratio of diarylethene to PFBT was as high as 20, which could make the PFBT nanoparticles very dim because of the low concentration of PFBT inside each individual nanoparticle.

To address these challenges, we describe here the synthesis of SP functionalized with hydroxyl groups (SP-OH) and a very bright polymer, poly[(9,9-dioctylfluorenyl-2,7-diyl)-*co*-(1,4-benzo-{2,1′,3}-thiadiazole)] functionalized with carboxyl groups (PFBT-COOH). The purpose is to covalently bind the photochromic dyes to the polymer matrices. These resulting Pdots show good reversible photomodulation with high on/off ratio, increased brightness, and small size. Furthermore, we conjugated streptavidin onto the surfaces of Pdots so that we could carry out specific cellular targeting via biotin-streptavidin interactions for fluorescence imaging and flow cytometry experiments. We believe this work have demonstrated the promising applicability of these photoswitchable Pdots in a wide range of cellular and imaging studies.

## RESULTS AND DISCUSSION

Our strategy was to create photoswitchable Pdots that exploited the light-controllable energy transfer from PFBT polymer to photochromic molecules conjugated to the PFBT polymer matrix itself. We also blended the carboxyl-terminated polystyrene polymer, PS-PEG-COOH, with the matrix of photochrome-conjugated PFBT polymer to increase the carboxylic functional groups of Pdots so that they could be tagged with biological molecules for specific cellular targeting applications (Scheme 1).

**Design of Photoswitchable Pdots.** We wanted to create a photoswitchable Pdot based on light-controllable energy transfer. The first step was to select a suitable donor−acceptor pair. We selected PFBT as a donor because we previously demonstrated that PFBT Pdots exhibited extraordinary fluorescence brightness, excellent photostability, and good biocompatibility.[43] To ensure an efficient energy transfer between PFBT and photochromes, we chose the photochromic couple SP/MC as the acceptor. SP does not absorb light above 420 nm, but its photogenerated form, MC, exhibits a high absorption centered at ~530 nm, which overlaps substantially with the emission spectrum of PFBT (Scheme 1B). To modulate the emission intensity of Pdots, we aimed to utilize FRET from the PFBT matrix (donor) to MC molecules (acceptor). More specifically, as shown in Scheme 1B, a short irradiation (5 s) of a 365 nm hand-held UV lamp (3.5 $\mu$W with a sample-source distance of ~1 cm) on the SP molecules caused the conversion of SP to MC along with the appearance of a high absorption band between 500 and 600 nm. As FRET efficiency depends on the degree of spectral overlap between the emission spectrum of the donor and the absorption spectrum of the acceptor, we expected that the MC could efficiently quench the fluorescence of PFBT because of the extensive spectral overlap between the absorption of MC and the emission of PFBT.

Scheme 1A illustrates our strategy for the preparation of photoswitchable Pdots. We first covalently bound SP molecules onto the fluorene moieties of PFBT in THF (see experimental section). After the reaction, a THF solution of the polystyrene copolymer, PS-PEG-COOH, was added and mixed well with the solution of spiropyran-bound PFBT (PFBT-SP). To form Pdots, the mixture was then injected into a water solution using nanoprecipitation under vigorous sonication. During Pdot formation, the hydrophobic polystyrene backbones were coprecipitated with hydrophobic PFBT polymer, while the PEG chains were used to minimize nonspecific adsorption and the carboxyl groups were used for bioconjugation reactions.

**Conjugation of SP to PFBT.** In an effort to covalently attach SP molecules onto PFBT, we first synthesized PFBT functionalized with carboxyl (PFBT-COOH) or amine groups (PFBT-$NH_2$). Then we synthesized SP functionalized with carboxyl (SP-COOH), amine (SP-$NH_2$), or hydroxyl groups


dx.doi.org/10.1021/ac302245t | *Anal. Chem.* 2012, 84, 9431−9438

(SP-OH; Figure S1). We tried several synthetic routes including the conjugations of PFBT-COOH to SP-$NH_2$, PFBT-COOH to SP-OH, and PFBT-$NH_2$ to SP-COOH in THF. However, we found that both the conjugations of PFBT-COOH to SP-$NH_2$ and PFBT-$NH_2$ to SP-COOH caused serious aggregation in the subsequent step of nanoprecipitation in water, probably due to the excessive amount of amine groups that might be present on the Pdot surface.[54] In contrast, as shown in Figure 1A, B, the conjugation of PFBT-COOH to SP-OH resulted in homogeneous and small particle sizes (average diameter of 16 nm) without any Pdot aggregation. It is worth mentioning that we also tried PFBT-COOH with lower molar fractions of carboxyl groups, but the FRET efficiency decreased. We attributed the weakened FRET to the decreased number of MC molecules (acceptor) conjugated onto PFBT side chains. To attach a sufficient amount of SP/MC onto PFBT, we synthesized PFBT functionalized with 50% of carboxyl groups; however, even higher molar fractions of carboxyl groups would make PFBT polymer water-soluble and difficult to form Pdots. As displayed in the bottom-right corner in Scheme 1A, gel electrophoresis showed that bare PFBT Pdots moved much faster toward the positive electrode than PFBT-SP Pdots and similarly sized PFBT-SP Pdots after streptavidin conjugation. This result indicated that the carboxyl groups on PFBT were consumed by SP and streptavidin, which resulted in less negative charges on these Pdot surfaces.

As illustrated in Scheme 1C, light induced a conformational change from SP to MC form and thus quenched the emission from PFBT via FRET. Figure 1C exhibits the absorption spectra of PFBT-SP Pdots before and after UV irradiation. From the inset, we can clearly see the emergence of the absorption peak at ~560 nm after UV light irradiation. We noted that MC absorption in PFBT Pdots (Figure 1C) revealed a red shift of ~30 nm compared to that in methanol (Scheme 1B). This red shift is attributed to the hydrophobic environment of PFBT, which also suggests that the MC molecules were successfully incorporated into the PFBT polymer matrix. The molecular weight of PFBT we synthesized here (Figure S1B) is ~14000, which means there are ~10 BT units per polymer chains. Based on this information and the molar extinction coefficient of MC and PFBT,[35,55] the number of MC per BT unit was calculated to be 8−10.

The PFBT-SP Pdots were then conjugated to streptavidin via 1-ethyl-3-[3-dimethylaminopropyl]carbodiimide hydrochloride (EDC)-catalyzed coupling for cellular labeling. We did not observe any leakage of SP molecules from the PFBT-SP-streptavidin conjugates after one month of storage at 4 °C because of the strong covalent bonds between PFBT and SP; this high stability could not be achieved by physical doping/blending of SP into PFBT.

**Fluorescence Photomodulation of PFBT-SP-Streptavidin Pdots.** We first characterized the efficiency and repeatability of the SP-OH photoswitching cycle in methanol. After the formation MC-OH, the efficiency of back photoconversion to SP-OH by excitation with visible light was found to be very close to unity (Figure S2A). The switching cycle could be repeated more than eight times without detectable photodegradation processes occurring (Figure S2B). A fluorescence peak centered at $\lambda_{max}$ = 630 nm was always observed after UV light irradiation and assigned to MC-OH, as confirmed by the excitation spectrum (Figure S2).

The fluorescence of PFBT-SP-streptavidin Pdots (at ~540 nm) was significantly quenched by the MC molecules generated after 1 min of UV irradiation ($\lambda$ = 365 nm, power = 3.5 $\mu$W); a small emission peak at ~650 nm also emerged (Figure 2A). Analogous to the methanol solutions, this new

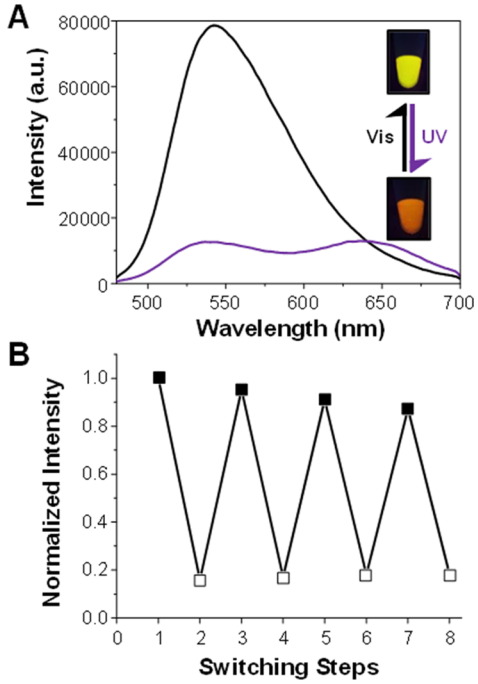


**Figure 2.** (A) Emission spectra of PFBT-SP-streptavidin Pdots in 20 mM HEPES buffer solution before (black line) and after (purple line) UV (365 nm) irradiation. The inset shows the photographs of Pdot solution before (upper image) and after (bottom image) a pulse of 365 nm UV irradiation. The photographs were taken within 1 s under a UV lamp. (B) Monitoring of cyclic photoconversion effects on the fluorescence intensity of PFBT-SP-streptavidin Pdots. Black squares represent the emission intensity of PFBT-SP-streptavidin Pdots after white light irradiation, while the open white squares represent the emission intensity of PFBT-SP-streptavidin Pdots after UV light (365 nm) irradiation. All data were recorded at 540 nm and excited at 450 nm.

signal was ascribed to the fluorescence of MC units. Its appearance demonstrated that the quenching of PFBT emission was caused by FRET toward MC, following the energy diagram shown in Scheme S1. Because this peak can be observed only in a hydrophobic environment,[30] it further confirmed that MC molecules were embedded inside PFBT polymer matrix during nanoparticle preparation, rather than exposed to the aqueous solution. The close proximity of MC quenchers to PFBT is beneficial for efficient FRET between the two.

The peak fluorescence of PFBT was quenched to only 14% of its original value by UV-generated MC and recovered almost all of its intensity when MC was converted back to SP by exposure to visible light (a mixture of light of wavelengths between 450 and 750 nm) for 5 min. This fluorescence photomodulation can be easily detected by the naked eye under a 365 nm UV lamp (Figure 2A). Figure 2B demonstrates that the photomodulation by switching back and forth between UV and visible irradiation could be repeated for multiple cycles with a slight decrease of fluorescence recovery. This sturdy cyclic photoconversion indicated minimal photodegradation of the photochrome and the semiconducting polymer. There was still nearly 90% of quenching efficiency after eight switching steps, demonstrating the fatigue-resistant property of SP/MC


dx.doi.org/10.1021/ac302245t | Anal. Chem. 2012, 84, 9431−9438

molecules. The suitability of these photoswitchable probes to microscopy and optical super-resolution imaging applications is also strongly dependent on their brightness ($B$).[56] Our Pdots are characterized by a very high absorption coefficient ($\varepsilon$ = 1.8 × 107 $M^{-1}$ $cm^{-1}$ at 450 nm for nanoparticles with a diameter of 15 nm), which makes them exceptionally bright probes ($B$ = 2.9 × $10^6$ $M^{-1}$ $cm^{-1}$), ensuring the achievement of high contrast level by the use of low excitation power. Other relevant photophysical parameters are reported in Table 1.

**Table 1. Emission Properties of PFBT-SP Pdots in Water before and after UV Irradiation, and MC-OH in Methanol after Exposure to UV Light[a]**

| probe | $\tau$ (ns) | $\Phi$ (%) | $\lambda_{max}$ (nm) | $\eta_{P-C}$ (%) |
|---|---|---|---|---|
| PFBT-SP Pdot | 3.4 | 18 | 540 | 90 |
| PFBT-SP Pdot[b] | 1.0 | | 540 | |
| MC-OH[b,c] | 0.21 | 1 | 646 | 100 |
| MC-OH[b,d] | | | 650 | |

[a]Fluorescence lifetime ($\tau$), quantum yield ($\Phi$), maximum wavelength of fluorescence emission ($\lambda_{max}$), and photo-conversion efficiency ($\eta_{P-C}$) are reported. $\eta_{P-C}$ reported for Pdots refers to the fluorescence photomodulation of PFBT. Notice that the decrease of PFBT lifetime after irradiation by UV light confirms the occurrence of a quenching mechanism consistent with FRET. MC-OH emission maximum in Pdot matrix was found after subtraction of PFBT's residual profile. Similar to its absorption profile, MC-OH fluorescence shows a red shift in Pdot matrix. [b]After UV irradiation. [c]In methanol solution. [d]Inside of the Pdot polymer matrix.

It is worth mentioning that all photomodulation experiments were performed at room temperature in a HEPES buffer solution without going through oxygen removal or degassing procedures. Our results demonstrate that our photoswitchable Pdots were very photostable and can be readily used for biological applications.

**Calculation of Förster Radius for PFBT-MC Pair.** Because the excitations of covalently bound MC is caused by FRET, knowledge of the FRET efficiency between PFBT and MC is important. FRET is a nonradiative dipole−dipole interaction, whose efficiency ($E$) is given by:

$$E = \left[1 + \left(\frac{r}{R_o}\right)^6\right]^{-1} \quad (1)$$

$$R_o^{\,6} = 8.79 \times 10^{-5}(\kappa^2 n^{-4} Q_D J) \quad (\text{in Å}) \quad (2)$$

where $r$ is the distance between the donor and the acceptor which, in our case, is the distance between PFBT and MC; $R_o$ is the Förster-like radius that represents a specific separation distance where the energy transfer efficiency is reduced to 50% of the maximal value; $\kappa^2$ is an orientation factor, which is set to 2/3 for a randomly orientated donor−acceptor pair in solution; $n$ is the refractive index of the medium, which is 1.85 for PFBT matrices in our experiments; $Q_D$ is the quantum yield of the donor in the absence of acceptors, which is 18% for PFBT Pdots; and $J$ is the spectral integral as a function of wavelength and expresses the degree of spectral overlap between the emission spectrum of the donor and the absorption spectrum of the acceptor. To obtain the value of $R_o$, first we had to calculate $J$ from the following equation:

$$J(\lambda) = \frac{\int_0^\infty F_D(\lambda)\varepsilon_A(\lambda)\lambda^4 d\lambda}{\int_0^\infty F_D(\lambda) d\lambda} \quad (\text{in } M^{-1}\ cm^{-1}\ nm^4) \quad (3)$$

where $F_D(\lambda)$ is the dimensionless emission intensity, $\lambda$ is the wavelength in units of nm, $\varepsilon_A(\lambda)$ is the molar absorption coefficient of MC.

Scheme 1B shows the degree of spectral overlap between the PFBT emission and the MC absorption. Based on this information, we calculated that $J$ was ~6.2 × $10^{13}$ $M^{-1}$ $cm^{-1}$ $nm^4$ using eq 3. The corresponding Förster radius, $R_o$, was determined to be ~2.0 nm using eq 2. Considering that the Förster radius for our PFBT donor-MC acceptor pair was relatively short, we got very efficient energy transfer inside the PFBT-SP Pdot system with an average particle size of 16 nm in diameter. This amplified energy transfer from PFBT to MC could be attributed to the covalent binding between the donor−acceptor pair that forces them into close proximity to facilitate FRET processes. We have also calculated FRET efficiency ($E$) according to eq 1 (see Supporting Information).

**Specific Labeling of Cellular Targets with Photoswitchable Pdots.** We next used the photoswitchable PFBT-SP-streptavidin Pdots for both cell-surface and subcellular labeling to evaluate the photoreversible cellular imaging. In one experiment, we used photoswitchable Pdots to label membrane proteins on MCF-7 cells. The PFBT-SP-streptavidin conjugates, along with primary biotin antihuman CD326 EpCAM antibody and biotinylated goat antimouse IgG secondary antibody, labeled the surfaces of live MCF-7 cells. The PFBT-SP-streptavidin Pdots specifically targeted the surface membrane of cells (Figure 3A). There was not any noticeable fluorescence signal from Pdots for the negative control sample (Figure 3B). To evaluate the photoswitching performance of Pdots in cells, we applied 5 s of UV light to the Pdot-labeled MCF-7 cells. Figure 3C shows that the fluorescence (green color) of Pdots was quenched by nearly 50% after 5 s of irradiation while the emission intensity of nuclear counterstain (blue color) remained unchanged. Moreover, the fluorescence of Pdots recovered to ~90% of its initial intensity after a 3 min period of white light (a mixture of light of wavelengths between 450 and 750 nm) irradiation, but the fluorescence of nuclear counterstain exhibited negligible change (Figure 3D). These results clearly demonstrated that SP/MC served as a great toggle switch for fluorescent Pdots, showing their promising potential for applications of biological imaging.

Additionally, we also carried out flow cytometry experiments showing that T lymphocyte cells could be specifically labeled with PFBT-SP-streptavidin Pdots (Figure S3). We also performed microtubule labeling inside HeLa cells where the biotinylated monoclonal anti-$\alpha$-tubulin antibody and PFBT-SP-streptavidin Pdots were sequentially incubated with the cells (Figure 4A). The microtubule subcellular labeling experiments in HeLa cells and the specific surface targeting on MCF-7 cells together demonstrate that these photoswitchable Pdots could be applied to various cell lines with highly specific binding activity and minimal nonspecific absorption. Photomodulation of PFBT-SP-streptavidin Pdots inside HeLa cells was also achieved (Figure 4B) where ~50% of Pdot fluorescence was quenched after UV light irradiation (Figure 4C). This photomodulation result is consistent with that shown with MCF-7 cells, suggesting that the fluorescence modulation of this new type of photoswitchable Pdots is applicable to various cell imaging applications.


dx.doi.org/10.1021/ac302245t | Anal. Chem. 2012, 84, 9431−9438

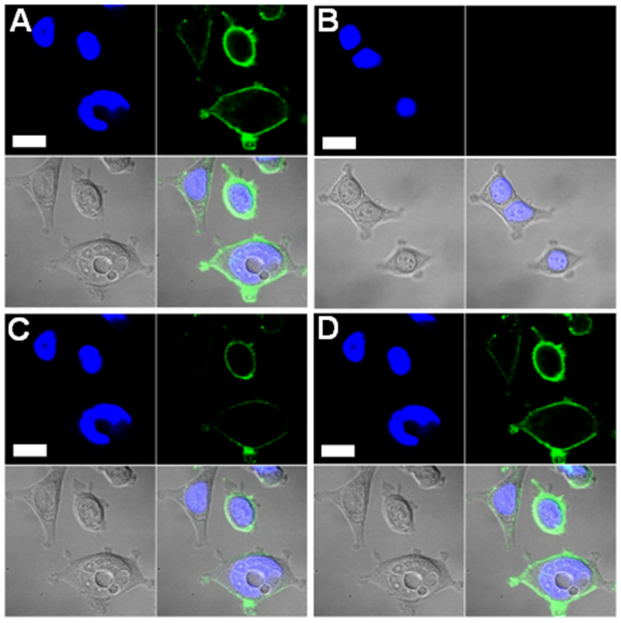


**Figure 3.** Confocal fluorescence images of MCF-7 cells labeled with PFBT-SP-streptavidin conjugates. The green fluorescence was from PFBT-SP-streptavidin and the blue fluorescence was from nuclear counterstain Hoechst 34580. The bottom-left and bottom-right panels of each image represent the Nomarski (DIC) and fluorescence overlaid with DIC images, respectively. The scale bars are 20 $\mu$m. (A) The clear fluorescence of labeled MCF-7 cells. (B) Images of a negative control sample in which the experiment was carried out under the same conditions as (A) except the secondary antibody was not added. (C) Images of labeled MCF-7 cells after irradiation with 365 nm UV light. (D) Images of labeled MCF-7 cells, as shown in (C), followed by a subsequent illumination of a white light.

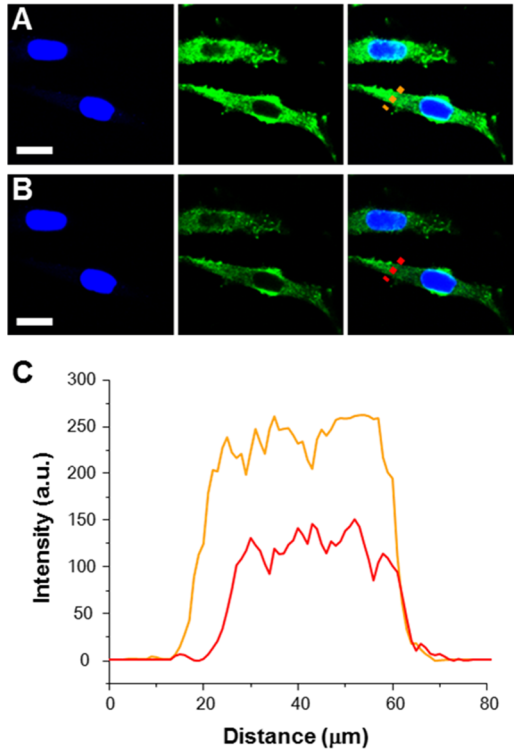


**Figure 4.** Confocal fluorescence images of microtubules labeled with PFBT-SP-streptavidin inside HeLa cells (A) before and (B) after UV light irradiation at 365 nm. The blue fluorescence is from nuclear counterstain Hoechst 34580 and the green fluorescence is from PFBT-SP-streptavidin Pdots. The right two panels show the fluorescence image overlays of blue and green fluorescence. The scale bars are 20 $\mu$m. (C) The cross-sectional plots of Pdot fluorescence as shown in (A; gold line) and (B; red line), where a ~50% quenching efficiency was observed after UV light irradiation.

## CONCLUSIONS

We report the reversible fluorescence photomodulation of PFBT-SP-streptavidin Pdots in which the SP was conjugated to the side chains of PFBT to facilitate the efficient energy transfer from PFBT to the photoinduced MC. In a typical experiment, 86% of PFBT emission intensity was quenched after UV light irradiation, and PFBT emission was recovered by irradiation with visible light; this photoswitching could be repeated for multiple cycles. We also demonstrated the bioconjugation of these photoswitchable Pdots and their highly specific binding to both cell surfaces and interiors. Moreover, the calculation of FRET efficiency indicates that this amplified energy transfer can be attributed to the covalent binding of SP to PFBT that keeps them in close proximity. These results, obtained by the use of low power lamps, clearly demonstrate that SP/MC served as a great toggle for fluorescent Pdots, showing their promising potential for applications in biological and super-resolution imaging.

## EXPERIMENTAL SECTION

**Materials.** The following chemicals were purchased from Sigma-Aldrich and used as received: 2,7-dibromofluorene, sodium hydroxide, *tert*-butyl 6-bromohexylcarbamate, tetrahydrofuran (THF; anhydrous, ≥99.9%, inhibitor-free), toluene, tetrabutylammonium bromide ($Bu_4NBr$), phenylboronic acid, bromobenzene, methanol, tetrakis(triphenylphosphine)palladium ($Pd(PPh_3)_4$), dichloromethane ($CH_2Cl_2$), 4,7-dibromobenzo[*c*]-1,2,5-thiadiazole, 9,9-dihexylfluorene-2,7-diboronic acid, bis(1,3-propanediol) ester, sodium carbonate, and hydrochloric acid. The chemical structures of poly[9,9-dioctylfluorenyl-2,7-diyl)-*co*-1,4-benzo-{2,1′-3}-thiadiazole)] (PFBT) functionalized with carboxyl groups and SP functionalized with hydroxyl groups are shown in Supporting Information. A comb-like polymer, polystyrene grafted with ethylene oxide functionalized with carboxyl groups (PS-PEG-COOH, main chain MW 8500, graft chain MW 1200, total chain MW 21700, polydispersity 1.25), was purchased from Polymer Source Inc. (Quebec, Canada) and used as received without further purification. All other chemical reagents were purchased from Invitrogen (Carlsbad, CA) and used as received. High purity water (18.2 MΩ·cm) was used throughout the experiment.

**Preparation of Photoswitchable (PFBT-SP) Pdots.** Typically, 2 mg of PFBT-COOH, 5 mg of SP-OH, 1 mg of 4-dimethylaminopyridine, and 5 mg of dicyclohexylcarbodiimide were added to 2 mL of THF solution in a vial. The reaction mixture was stirred for 12 h at room temperature and then stored at −20 °C until further usage. After that, 200 $\mu$L of PFBT-SP conjugates, 20 $\mu$L of PS-PEG-COOH (2 mg/mL in THF) were added into 5 mL of THF. This mixture was then quickly injected into 10 mL of water under vigorous sonication. THF was then removed by purging with nitrogen on a 96 °C hot plate for 1 h. The resulting Pdot solution was filtered through a 0.2 $\mu$m cellulose acetate membrane filter to remove any aggregates formed during preparation.


dx.doi.org/10.1021/ac302245t | *Anal. Chem.* 2012, 84, 9431−9438

**Bioconjugation and Characterization of Photoswitchable Pdots.** Bioconjugation was performed by using the EDC-catalyzed reaction between carboxylate-functionalized PFBT-SP Pdots and the respective amine-containing streptavidin. Typically, 80 $\mu$L of polyethylene glycol (5% w/v PEG, MW 3350) and 80 $\mu$L of concentrated HEPES buffer (1 M) were added to 4 mL of Pdot solution, resulting in a Pdot solution in 20 mM HEPES buffer with a pH of 7.3. Then, 240 $\mu$L of streptavidin (1 mg/mL) was added to the solution and mixed on a vortex. After that, 80 $\mu$L of freshly prepared EDC solution (5 mg/mL in Milli-Q water) was added to the solution, and the mixture was stirred for 4 h at room temperature. After bionconjugation, 80 $\mu$L of BSA (10 wt %) was added to the Pdot solution and the reaction was continued for another 20 min. A 80 $\mu$L aliquot of Triton X-100 in Milli-Q water (2.5 wt %) was added to the Pdot-streptavidin mixture. The mixture was then transferred to a centrifugal ultrafiltration tube (Amicon Ultra-4, MWCO: 100 kDa) and then concentrated to 0.5 mL by centrifugation. Finally, the Pdot-Qdot-streptavidin bioconjugates were purified by gel filtration using Sephacryl HR-300 gel media.

The average particle size was determined by dynamic light scattering and transmission electron microscopy (TEM) to be 16 nm in diameter for PFBT-SP-streptavidin Pdots. For TEM, a drop of Pdot aqueous solution was placed onto a carbon-coated grid and allowed to evaporate at room temperature. TEM images of the synthesized Pdots were acquired using a FEI Tecnai F20 transmission electron microscope at an acceleration voltage of 200 kV. The absorption spectra of Pdot-Qdot NPs were measured by UV−visible spectroscopy (DU 720, Beckman Coulter, Inc., CA, U.S.A.). The fluorescence spectra were collected using a Fluorolog-3 fluorometer (HORIBA Jobin Yvon, NJ, U.S.A.). Fluorescence quantum yield of Pdots was determined by an integrating sphere (Model C9920-02, Hamamatsu Photonics) under 450 nm excitation from a 150 W CW Xenon lamp.

**Cell Culture and Labeling.** The cervical cancer cell line HeLa, white blood cell line T lymphocyte Jurkat, and breast cancer cell line MCF-7 were ordered from American Type Culture Collection (ATCC, Manassas, VA, U.S.A.). Primary cultured HeLa cells were grown in Dulbecco's modified Eagle medium (cat. no. 11885, Invitrogen) supplemented with 10% fetal bovine serum and 1% penicillin-streptomycin solution (5000 units/mL penicillin G, 50 $\mu$g/mL streptomycin sulfate in 0.85% NaCl) at 37 °C with 5% $CO_2$ humidified atmosphere. Jurkat T cells were cultured at 37 °C, 5% $CO_2$ in RPMI 1640 medium supplemented with 10% fetal bovine serum (FBS) and 1% penicillin-streptomycin solution. The cells were precultured in a T-75 flask and allowed to grow for 5−7 days prior to experiments until ∼80% confluence was reached. To prepare cell suspensions, the adherent cancer cells were quickly rinsed with media and then incubated in 5 mL trypsin-ethylenediaminetetraacetic (EDTA) solution (0.25 w/v % trypsin, 0.25 g/L EDTA) at 37 °C for 5 min. The cell suspension solution was then centrifuged at 6000 rpm for 10 min to precipitate the cells to the bottom of the tube. After taking out the upper media, the cells was rinsed and resuspended in 5 mL of culture media. Approximately $10^5$ cells were split onto a glass-bottomed culture dish and allowed to grow for 12 h before Pdot tagging. Prior to fluorescence imaging, the cells were rinsed with PBS buffer to remove any nonspecifically bound Pdots on the cell surface.

For cell labeling experiments, BlockAid blocking buffer was purchased from Invitrogen (Eugene, OR, U.S.A.). For labeling cell-surface markers with IgG, a million MCF-7 cells in 100 $\mu$L labeling buffer (1× PBS, 2 mM EDTA, 1% BSA) was incubated with 0.3 $\mu$L of 0.5 mg/mL primary biotin antihuman CD326 EpCAM antibody (eBioScience, San Diego, CA, U.S.A.) on a rotary shaker in the dark and at room temperature for 30 min, followed by a washing step using labeling buffer. Then the cells were incubated with 1.5 nM Pdot-SP-streptavidin conjugates in BlockAid buffer for 30 min on a shaker in the dark and at room temperature, followed by two washing steps with labeling buffer. Prior to cell incubation, Pdot-SP solutions were sonicated for 3 min to disperse any potential aggregates. Negative controls were obtained by incubating cells with Pdot-SP-streptavidin conjugates in the absence of primary biotinylated antibody. Cell fixation was performed by dissolving the cell pellet obtained by centrifugation in 500 $\mu$L of fixing buffer (1× PBS, 2 mM EDTA, 1% BSA, 1% PFA).

Flow cytometry measurements were performed on fresh samples with $10^6$ cells/0.5 mL and prepared following the procedure previously described. The flow cytometer LSRII (BD Bioscience, San Jose, CA U.S.A.) was used: Cells flowing in the detection chamber were hit with a 488 nm laser beam, side- and forward-scattered light and fluorescence emission were collected, the latter was filtered by a 505 long-pass and a 530/30 band-pass, and all signals were detected by PMT arrays. Representative populations of cells were chosen by selection of an appropriate gate. Detection of cell fluorescence was continued until at least 104 events had been collected in the active gate.

For microtubule-labeling experiments, about $10^5$ thousands of HeLa cells were plated on a 22 × 22 mm glass coverslip and cultured until the density reached 60−70% confluence. The cells were fixed with 4% paraformaldehyde for 10 min, permeabilized with 0.25% Triton-X 100 in PBS buffer for 15 min, and then blocked in BlockAid blocking buffer for another 30 min. The fixed and blocked HeLa cells were subsequently incubated with 5 $\mu$g/mL biotinylated monoclonal anti-$\alpha$-tubulin antibody (Biolegend, San Diego, CA, U.S.A.) for 60 min and then Pdot-SP-streptavidin conjugates for 30 min. The Pdot-SP labeled cells were then counterstained with Hoechst 34580 and imaged immediately on a fluorescence confocal microscope (Zeiss LSM 510).

**Cell Imaging.** The fluorescence spectra of Pdot-tagged cells were acquired with a fluorescence confocal microscope (Zeiss LSM 510) under ambient conditions (24 ± 2 °C). The confocal fluorescence images were collected using a diode laser at 488 nm (∼15 mW) as the excitation source and an integration time of 1.6 $\mu$s/pixel. A Carl Zeiss 63x ("C-Apochromat" 63×/1.2 W Corr) objective was utilized for imaging and spectral data acquisition; the laser was focused to a spot size of ∼5 $\mu m^2$.

## ■ ASSOCIATED CONTENT

### Supporting Information

We have included the following information: (1) Chemical structures of PFBT and SP derivatives, (2) Repeatability of SP-OH photoswitching cycle, (3) Schematic energy level diagram of PFBT and MC, and (4) Flow cytometry detection of PFBT-SP-streptavidin labeled T lymphocyte (Jurkat) cells. This material is available free of charge via the Internet at http://pubs.acs.org.


dx.doi.org/10.1021/ac302245t | Anal. Chem. 2012, 84, 9431−9438

## AUTHOR INFORMATION


### Corresponding Author

*E-mail: chiu@chem.washington.edu.

### Author Contributions

†Both authors contributed equally to this work.


### Notes

The authors declare no competing financial interest.

## ACKNOWLEDGMENTS

D.T.C. gratefully acknowledges support for this research from the National Institutes of Health (GM085485). We also acknowledge support from the Keck Imaging Center, the Cell Analysis Facility, and Center for Nanotechnology at the University of Washington for use of instruments.

## REFERENCES


(1) Sancar, A.; Lindsey-Boltz, L. A.; Ünsal-Kaçmaz, K.; Linn, S. *Annu. Rev. Biochem.* **2004**, *73*, 39−85.

(2) Fritzsch, F. S. O.; Dusny, C.; Frick, O.; Schmid, A. *Annu. Rev. Chem. Biomol. Eng.* **2012**, *3*, 129−155.

(3) Que, E. L.; Domaille, D. W.; Chang, C. J. *Chem. Rev.* **2008**, *108*, 1517−1549.

(4) Thomas, S. W.; Joly, G. D.; Swager, T. M. *Chem. Rev.* **2007**, *107*, 1339−1386.

(5) Thompson, R. B. *Fluorescence Sensors and Biosensors*; CRC Press: Boca Raton, FL, 2006.

(6) Hell, S. W.; Wichmann, J. *Opt. Lett.* **1994**, *19*, 780−782.

(7) Rittweger, E.; Han, K. Y.; Irvine, S. E.; Eggeling, C.; Hell, S. W. *Nat. Photon.* **2009**, *3*, 144−147.

(8) Gustafsson, M. G. L. *Proc. Natl. Acad. Sci. U.S.A.* **2005**, *102*, 13081−13086.

(9) Rust, M. J.; Bates, M.; Zhuang, X. *Nat. Methods* **2006**, *3*, 793−795.

(10) Betzig, E.; Patterson, G. H.; Sougrat, R.; Lindwasser, O. W.; Olenych, S.; Bonifacino, J. S.; Davidson, M. W.; Lippincott-Schwartz, J.; Hess, H. F. *Science* **2006**, *313*, 1642−1645.

(11) Ando, R.; Mizuno, H.; Miyawaki, A. *Science* **2004**, *306*, 1370−1373.

(12) Gust, D.; Andréasson, J.; Pischel, U.; Moore, T. A.; Moore, A. L. *Chem. Commun.* **2012**, *48*, 1947−1957.

(13) Irie, M.; Fukaminato, T.; Sasaki, T.; Tamai, N.; Kawai, T. *Nature* **2002**, *420*, 759−760.

(14) Bianco, A.; Perissinotto, S.; Garbugli, M.; Lanzani2, G.; Bertarelli, C. *Laser Photonics Rev.* **2011**, *5*, 711−736.

(15) Chen, J.; Zeng, F.; Wu, S.; Su, J.; Tong, Z. *Small* **2009**, *5*, 970−978.

(16) Chen, J.; Zeng, F.; Wu, S.; Chen, Q.; Tong, Z. *Chem.—Eur. J.* **2008**, *14*, 4851−4860.

(17) Wu, T.; Zou, G.; Hu, J.; Liu, S. *Chem. Mater.* **2009**, *21*, 3788−3798.

(18) Fölling, J.; Polyakova, S.; Belov, V.; Blaaderen, A. v.; Bossi, M. L.; Hell, S. W. *Small* **2008**, *4*, 134−142.

(19) Diaz, S. A.; Menendez, G. O.; Etchehon, M. H.; Giordano, L.; Jovin, T. M.; Jares-Erijman, E. A. *ACS Nano* **2011**, *5*, 2795−2805.

(20) Jeong, J.; Yun, E.; Choi, Y.; Jung, H.-y.; Chung, S. J.; Song, N. W.; Chung, B. H. *Chem. Commun.* **2011**, *47*, 10668−10670.

(21) Genovese, D.; Montalti, M.; Prodi, L.; Rampazzo, E.; Zaccheroni, N.; Tosic, O.; Altenhöner, K.; May, F.; Mattay, J. *Chem. Commun.* **2011**, *47*, 10975−10977.

(22) Chen, J.; Zhang, P.; Fang, G.; Yi, P.; Yu, X.; Li, X.; Zeng, F.; Wu, S. *J. Phys. Chem. B* **2011**, *115*, 3354−3362.

(23) Yildiz, I.; Impellizzeri, S.; Deniz, E.; McCaughan, B.; Callan, J. F.; Raymo, F. M. *J. Am. Chem. Soc.* **2011**, *133*, 871−879.

(24) Tomasulo, M.; Yildiz, I.; Raymo, F. M. *Aust. J. Chem.* **2006**, *59*, 157−178.

(25) Medintz, I. L.; Trammell, S. A.; Mattoussi, H.; Mauro, J. M. *J. Am. Chem. Soc.* **2004**, *126*, 30−31.

(26) Derfus, A. M.; Chan, W. C. W.; Bhatia, S. N. *Nano Lett.* **2004**, *4*, 11−18.

(27) Liu, Y.-S.; Sun, Y.; Vernier, P. T.; Liang, C.-H.; Chong, S. Y. C.; Gundersen, M. A. *J. Phys. Chem. C* **2007**, *111*, 2872−2878.

(28) Michalet, X.; Pinaud, F. F.; Bentolila, L. A.; Tsay, J. M.; Doose, S.; Li, J. J.; Sundaresan, G.; Wu, A. M.; Gambhir, S. S.; Weiss, S. *Science* **2005**, *307*, 538−544.

(29) Sapsford, K. E.; Pons, T.; Medintz, I. L.; Mattoussi, H. *Sensors* **2006**, *6*, 925−953.

(30) Zhu, M.-Q.; Zhu, L.; Han, J. J.; Wu, W.; Hurst, J. K.; Li, A. D. Q. *J. Am. Chem. Soc.* **2006**, *128*, 4303−4309.

(31) Zhu, L.; Wu, W.; Zhu, M.-Q.; Han, J. J.; Hurst, J. K.; Li, A. D. Q. *J. Am. Chem. Soc.* **2007**, *129*, 3524−3526.

(32) Hu, D.; Tian, Z.; Wu, W.; Wan, W.; Li, A. D. Q. *J. Am. Chem. Soc.* **2008**, *130*, 15279−15281.

(33) Tian, Z.; Wu, W.; Wan, W.; Li, A. D. Q. *J. Am. Chem. Soc.* **2009**, *131*, 4242−4252.

(34) Tian, Z.; Li, A. D. Q.; Hu, D. *Chem. Commun.* **2011**, *47*, 1258−1260.

(35) Wu, C.; Bull, B.; Szymanski, C.; Christensen, K.; McNeill, J. *ACS Nano* **2008**, *2*, 2415−2423.

(36) Tian, Z.; Yu, J.; Wu, C.; Szymanski, C.; McNeill, J. *Nanoscale* **2010**, *2*, 1999−2011.

(37) Pecher, J.; Mecking, S. *Chem. Rev.* **2010**, *110*, 6260−6279.

(38) Kaeser, A.; Schenning, A. P. H. J. *Adv. Mater.* **2010**, *22*, 2985−2997.

(39) Tuncel, D.; Demir, H. V. *Nanoscale* **2010**, *2*, 484−494.

(40) Li, K.; Liu, B. *J. Mater. Chem.* **2012**, *22*, 1257−1264.

(41) Pu, K.-Y.; Liu, B. *Adv. Funct. Mater.* **2011**, *21*, 3408−3423.

(42) Wu, C.; Jin, Y.; Schneider, T.; Burnham, D. R.; Smith, P. B.; Chiu, D. T. *Angew. Chem., Int. Ed.* **2010**, *49*, 9436−9440.

(43) Wu, C.; Schneider, T.; Zeigler, M.; Yu, J.; Schiro, P. G.; Burnham, D. R.; McNeill, J. D.; Chiu, D. T. *J. Am. Chem. Soc.* **2010**, *132*, 15410−15417.

(44) Wu, C.; Hansen, S. J.; Hou, P. Q.; Yu, J.; Zeigler, M.; Jin, Y.; Burnham, D. R.; McNeill, J. D.; Olson, J. M.; Chiu, D. T. *Angew. Chem., Int. Ed.* **2011**, *50*, 3430−3434.

(45) Chan, Y.-H.; Wu, C.; Ye, F.; Jin, Y.; Smith, P. B.; Chiu, D. T. *Anal. Chem.* **2011**, *83*, 1448−1455.

(46) Chan, Y.-H.; Jin, Y.; Wu, C.; Chiu, D. T. *Chem. Commun.* **2011**, *47*, 2820−2822.

(47) Ye, F.; Wu, C.; Jin, Y.; Chan, Y.-H.; Zhang, X.; Chiu, D. T. *J. Am. Chem. Soc.* **2011**, *133*, 8146−8149.

(48) Jin, Y.; Ye, F.; Zeigler, M.; Wu, C.; Chiu, D. T. *ACS Nano* **2011**, *5*, 1468−1475.

(49) Harbron, E. J.; Davis, C. M.; Campbell, J. K.; Allred, R. M.; Kovary, M. T.; Economou, N. J. *J. Phys. Chem. C* **2009**, *113*, 13707−13714.

(50) Davis, C. M.; Childress, E. S.; Harbron, E. J. *J. Phys. Chem. C* **2011**, *115*, 19065−19073.

(51) Peng, J.; He, X.; Wang, K.; Tan, W.; Wang, Y.; Liu, Y. *Anal. Bioanal. Chem.* **2007**, *388*, 645−654.

(52) Peng, H.-s.; Stolwijk, J. A.; Sun, L.-N.; Wegener, J.; Wolfbeis, O. S. *Angew. Chem., Int. Ed.* **2010**, *49*, 4246−4249.

(53) Osakada, Y.; Hanson, L.; Cui, B. *Chem. Commun.* **2012**, *48*, 3285−3287.

(54) Clafton, S. N.; Beattie, D. A.; Mierczynska-Vasilev, A.; Acres, R. G.; Morgan, A. C.; Kee, T. W. *Langmuir* **2010**, *26*, 17785−17789.

(55) Calvert, J. G.; Pitts, J. N. *Photochemistry*; Wiley: New York, 1966.

(56) Patterson, G.; Davidson, M.; Manley, S.; Lippincott-Schwartz, J. *Annu. Rev. Phys. Chem.* **2010**, *61*, 345−367.